# Hydrometeorological daily recharge assessment model (DREAM) for the Western Mountain Aquifer, Israel: Model application and effects of temporal patterns

N. A. Sheffer,[1,2] E. Dafny,[1] H. Gvirtzman,[1] S. Navon,[3] A. Frumkin,[3] and E. Morin[3]

Received 25 November 2008; revised 12 October 2009; accepted 3 November 2009; published 11 May 2010.

[1] Recharge is a critical issue for water management. Recharge assessment and the factors affecting recharge are of scientific and practical importance. The purpose of this study was to develop a daily recharge assessment model (DREAM) on the basis of a water balance principle with input from conventional and generally available precipitation and evaporation data and demonstrate the application of this model to recharge estimation in the Western Mountain Aquifer (WMA) in Israel. The WMA (area 13,000 $km^2$) is a karst aquifer that supplies 360–400 $Mm^3\ yr^{-1}$ of freshwater, which constitutes 20% of Israel's freshwater and is highly vulnerable to climate variability and change. DREAM was linked to a groundwater flow model (FEFLOW) to simulate monthly hydraulic heads and spring flows. The models were calibrated for 1987–2002 and validated for 2003–2007, yielding high agreement between calculated and measured values ($R^2$ = 0.95; relative root-mean-square error = 4.8%; relative bias = 1.04). DREAM allows insights into the effect of intra-annual precipitation distribution factors on recharge. Although annual precipitation amount explains ~70% of the variability in simulated recharge, analyses with DREAM indicate that the rainy season length is an important factor controlling recharge. Years with similar annual precipitation produce different recharge values as a result of temporal distribution throughout the rainy season. An experiment with a synthetic data set exhibits similar results, explaining ~90% of the recharge variability. DREAM represents significant improvement over previous recharge estimation techniques in this region by providing near-real-time recharge estimates that can be used to predict the impact of climate variability on groundwater resources at high temporal and spatial resolution.

**Citation:** Sheffer, N. A., E. Dafny, H. Gvirtzman, S. Navon, A. Frumkin, and E. Morin (2010), Hydrometeorological daily recharge assessment model (DREAM) for the Western Mountain Aquifer, Israel: Model application and effects of temporal patterns, *Water Resour. Res.*, *46*, W05510, doi:10.1029/2008WR007607.

## 1. Introduction

[2] Increasing water demand for an expanding population and related enhanced food and biofuel production on the one hand and reducing water supplies at a global scale on the other require improved management of water resources [e.g., *Lundqvist and Gleick*, 2000; *Vorosmarty et al.*, 2000; *Scanlon and Cook*, 2002]. Traditionally, water resources focused primarily on surface water; however, declining surface water resources has resulted in a shift toward increased use of groundwater resources because groundwater is readily available in most regions, such as the North China Plain, western India, and southern Asia [*Shah et al.*, 2000].

[3] Recharge is the process of adding water to an aquifer by percolating water through the soil and rock column [*Freeze and Cherry*, 1979; *Tindall and Kunkel*, 1999]. Recharge can vary spatially and temporally. Similar amounts of precipitation can result in different aquifer recharge rates as a function of the spatial and temporal distribution of precipitation (e.g., location of the storm core, number of wet and dry periods and also as a function of duration of wet periods) and morphoclimatic conditions (e.g., temperature, land use, vegetation, soil and rock types, and slope degree and aspect). For example, annual precipitation of 600 mm produces a 25%–35% recharge in the central mountains of Israel [*Gvirtzman*, 2002] but only a 5%–10% recharge in the Edwards aquifer of Texas [e.g., *Abbott*, 1975], which has apparently similar lithological, hydrological, and morphological characteristics. The main cause for the difference in recharge rates may be related to variations in the temporal distribution of precipitation: winter precipitation in Israel versus an annual distribution in Texas.

[4] The objectives of the current study were (1) to assess recharge processes and develop quantitative estimates of recharge rates for the regional Western Mountain Aquifer (WMA) (Figure 1) in Israel by constructing a distributed

[1]Institute of Earth Sciences, Hebrew University of Jerusalem, Jerusalem, Israel.
[2]Bureau of Economic Geology, University of Texas at Austin, Austin, Texas, USA.
[3]Department of Geography, Hebrew University of Jerusalem, Jerusalem, Israel.


0043-1397/10/2008WR007607

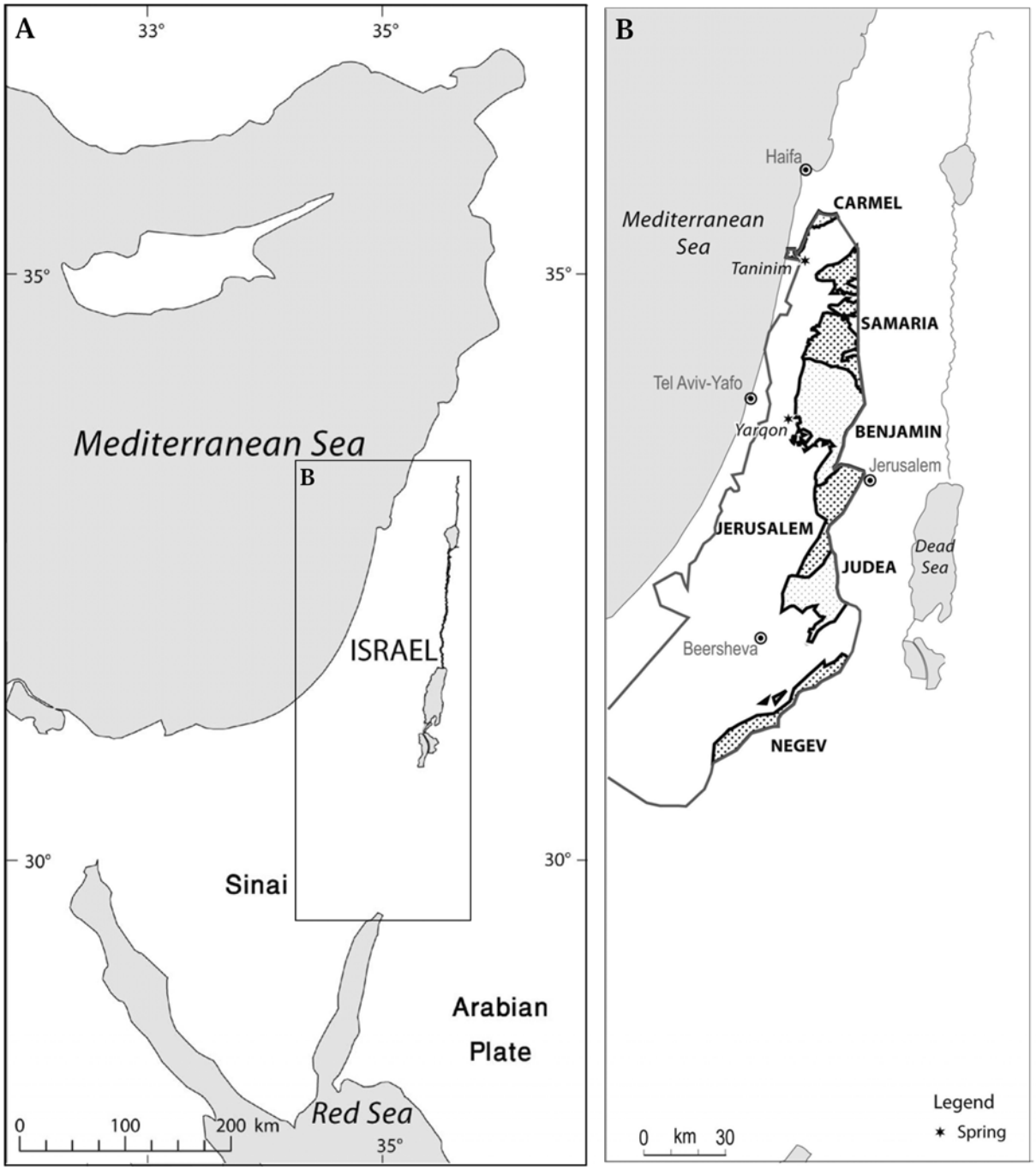


**Figure 1.** (a) Location map. (b) The whole Western Mountain Aquifer (WMA) (11,800 km$^2$; the phreatic and confined zones are outlined) and the six subbasins of the WMA recharge zone (2200 km$^2$, dotted areas). These subbasins are separated by structural and hydrological water divides. The two main spring outlets of the WMA (stars) are the Taninim in the north, draining the Carmel and Samaria subbasins, and the Yarqon in the center, draining the Benjamin, Jerusalem, Judea, and Negev subbasins.

hydrometeorological precipitation-recharge model based on a daily water budget and (2) to study the effect of a variety of temporal precipitation distributions on recharge to the aquifer.

[5] Recharge estimation is critical for assessing water availability and evaluating contaminant transport. Choosing appropriate techniques for quantifying groundwater recharge is complicated. *Scanlon et al.* [2002] reviewed various methods (Figure 2) and suggested choosing an adequate approach for recharge estimation according to (1) recharge rate, (2) aquifer area, and (3) recharge time scale. Keeping these considerations in mind, we found that the most appropriate technique for estimating recharge was a daily soil water balance model for a regional karst aquifer in the eastern Mediterranean with a recharge area of $\geq$1000 km$^2$, recharge rates of 100–1000 mm yr$^{-1}$, and recharge times of a few weeks to a few

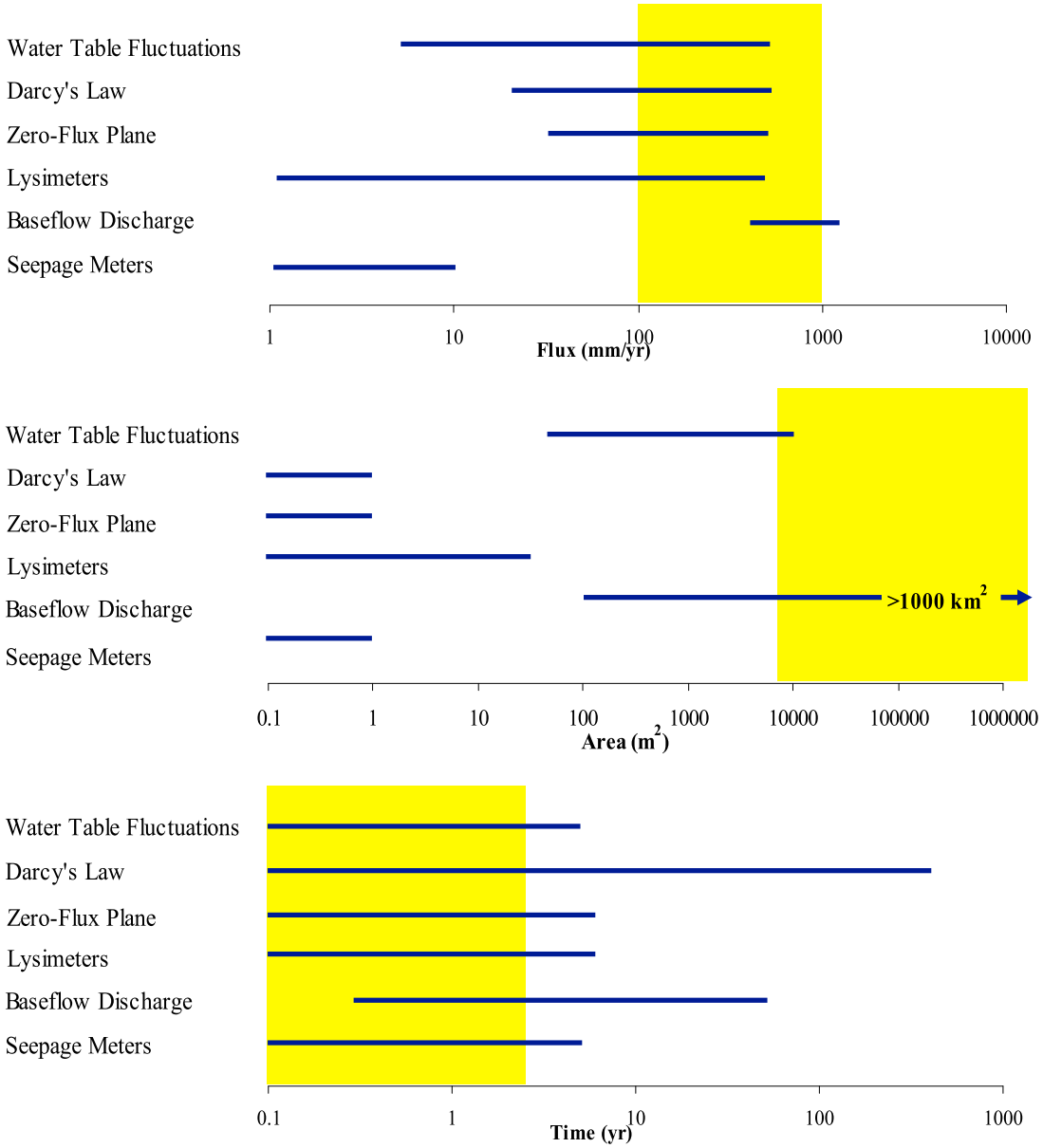


**Figure 2.** Range of fluxes, spatial scales, and time periods of recharge to aquifers that can be estimated by different techniques [*Scanlon et al.*, 2002]. The shading represents the flux, area, and time span relevant to this study.

months. The water balance model relates climatic forcing to water table fluctuations and base flow discharge to springs (Figure 2). Other techniques may also be suitable for this type of aquifer, such as applied tracer experiments; however, data availability is limited to daily precipitation and evaporation measurements and monthly groundwater table elevations and spring discharge.

[6] Recharge modeling based on soil water balance, as suggested by *Scanlon et al.* [2002], has recently been conducted for large-scale regional aquifers, such as the Basin of Mexico [*Carrera-Hernandez and Gaskin*, 2008], the Sultanate of Oman [*Rajmohan et al.*, 2007], Taiwan [*Lee et al.*, 2006], Iran [*Khazaei et al.*, 2003], and, in the United States, Kansas [*Sophocleous*, 2004, 2005], Minnesota [*Delin et al.*, 2007], Nebraska [*Szilagyi et al.*, 2005], and Nevada [*Flint et al.*, 2002]. In Israel, *Rimmer and Salingar* [2006] constructed a recharge model for the upper catchments of the Jordan River (Hydrological Model for Karst Environment (HAYMKE)). *Scanlon et al.* [2006] compiled recharge rates for $\geq$100 studies globally.

[7] This study presents the Daily Recharge Assessment Model (DREAM), which uses relatively high temporal resolution data to estimate recharge and, when linked with groundwater flow model, groundwater levels. This model allows a better understanding of the effect of temporal distribution of precipitation on recharge. By using DREAM it is possible to analyze and compare years with similar annual precipitation values but various intraseasonal distributions and to gain new insights on the most important factors affecting recharge. The paper is the first in a series of papers


**Figure 3.** The WMA recharge zone lithology. The area was divided into two main rock types: (1) limestone/dolomite areas, assigned $\mu_1$ values, and (2) chalk/marl areas, assigned $\mu_2$ values.

discussing insights derived using the DREAM [*Sheffer*, 2009]. In this paper DREAM is applied to the regional Israeli Western Mountain Aquifer. *Sheffer* [2009] describes other applications of DREAM on local-scale study sites of perched aquifers.

## 2. Western Mountain Aquifer (WMA)

[8] The WMA (also known as the Yarqon-Taninim Groundwater Basin, after its two main outlets: Yarqon and Taninim springs) provides approximately 20% of the freshwater supply for Israel [*Gvirtzman*, 2002]. It is divided into a western confined part, under the lowland and coastal plain (11,800 km$^2$), and an eastern phreatic part, over the mountain ranges (2200 km$^2$; Figure 1). The recharge areas lie beneath the Samarian and Judean mountains, Carmel Mountain, and a small area in the northern Negev [*Dafny et al.*, 2008a].

### 2.1. Aquifer Characteristics

[9] The aquifer is made up of carbonate rocks of the Judea Group (Albian-Turonian age [*Arkin*, 1967]). The Judea Group rocks are mainly limestone and dolomite, with relatively thin marl horizons and some chalk units (Figure 3). The main soil types in the recharge area are terra rossa and rendzina, typical soils developed on carbonate rocks in a Mediterranean climate [*Committee on Soil Classification*, 1979] (Figure 4). They comprise clay aggregates with a thickness of 0–0.25 m for rendzina and up to 1 m (in depressions) for terra rossa [*Dan and Koyumdjisky*, 1963; *Singer et al.*, 1998]. Desert deposits and soils (mainly loess) cover the southern parts (Figure 4) and restrict recharge due to swelling and sealing processes when moistened [*Dan and Koyumdjisky*, 1963; *Singer et al.*, 1998].

[10] The recharge area is characterized by steep, bare hillsides in the Judean and Samarian areas partially covered with cropland. Apart from urban areas of the nine main cities, most of the recharge zone is characterized by sparse villages (built-up area covers about 7% of the recharge area), forest in the northern recharge area (2.5%), and desert in the southern recharge area (semiarid to arid climate, 13%).

[11] Due to folding, uplift, and erosion processes, the Judea Group is exposed in the Judean and Samarian mountains and in the northern Negev desert, forming the recharge area of the WMA. These rocks have a well-developed fracture and karst system. Long-term water table stability of the aquifer in the past allowed development of karst features, mostly under saturated conditions [*Natan*, 2001; *Frumkin and Fischhendler*, 2005]. The aquifer thickness varies from 1000 m in the north and center to 500 m in the south [*Ben Gai et al.*, 2007]. The WMA is structurally continuous across the ridge, favoring development of a continuous piezometric surface with long and stable flow paths under phreatic and confined conditions. The WMA can be divided into two subbasins according to historical discharge zones: Taninim in the north and Yarqon in the center (Figure 1). The area can be further subdivided based on structural and hydrological water divides: Carmel and Samaria in the north drain into the Taninim spring, and Benjamin, Jerusalem, Judea, and Negev in the center and south drain into the Yarqon spring (Figure 1). A thorough description of the WMA is given by *Dafny et al.* [2008a].

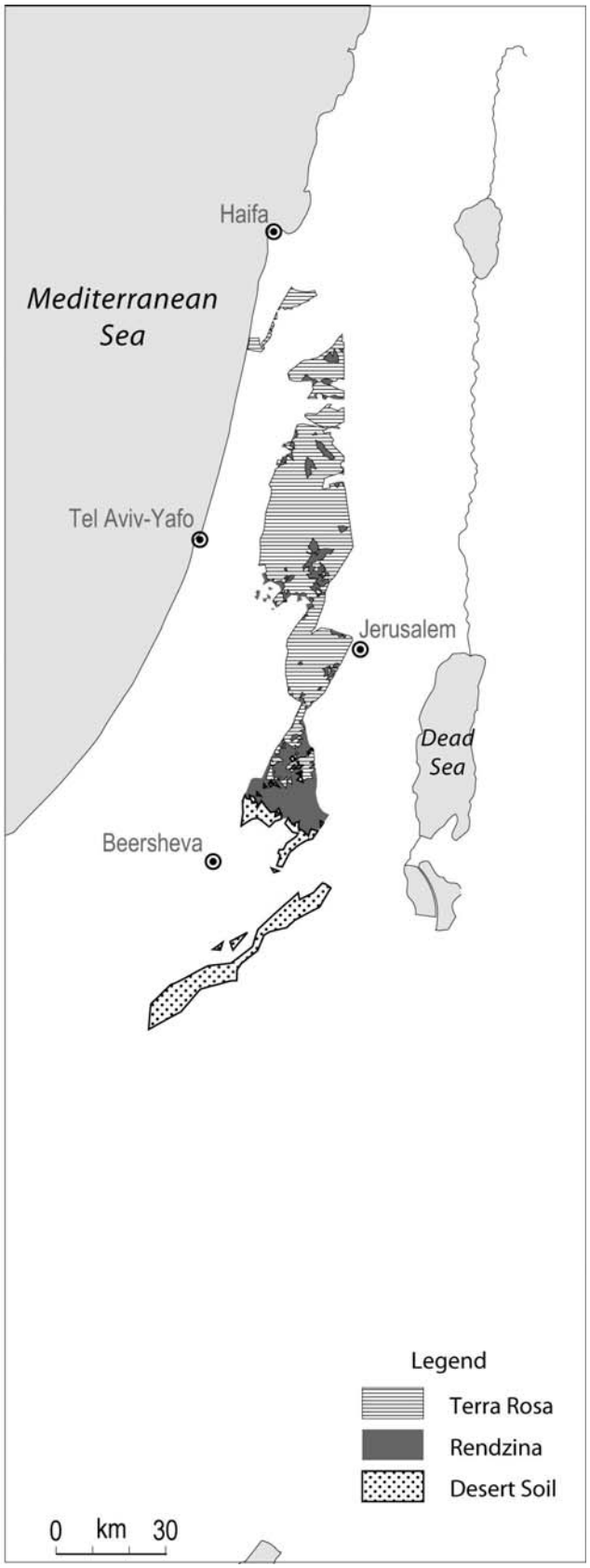


**Figure 4.** The WMA recharge zone pedology. The area was divided into three main soil types: (1) terra rossa areas, assigned $Z_1$ values; (2) rendzina areas, assigned $Z_2$ values; and (3) desert soil areas, assigned $Z_3$ values.

### 2.2. Climate

[12] Israel has a Mediterranean climate characterized by long, hot, dry summers and cool, wet winters, as modified locally by altitude and latitude. Precipitation is unevenly distributed, decreasing sharply southward (Figure 5) from mean annual precipitation of 700 mm in the northern recharge areas to $\leq$100 mm in the far south. The rainy season extends from October to early May, and precipitation peaks in December–February. About 70% of mean annual precipitation falls within November–March [*Goldreich*, 1998].

[13] Mean annual precipitation (MAP) over the WMA recharge area is ~550 mm, with the driest and wettest years on record (1860–2008) producing $\leq$250 mm and $\geq$1000 mm precipitation, respectively (according to the Israeli Meteorological Service records). The highest annual precipitation on record was in 1991, with annual precipitation approximately double the MAP in the WMA recharge area. (The years given herein are hydrological years; 1991 spans from 1 October 1991 to 30 September 1992.) The mean annual potential evaporation ranges from 1400 to 1800 mm, and the mean annual actual evapotranspiration (ET) over the WMA is estimated to be 65%–75% of annual precipitation [*Goldreich*, 1998; *Gvirtzman*, 2002]. Runoff values range from 3% to 6% of annual precipitation. According to measurements by the Israeli Hydrological Service (IHS), annual runoff as high as 12% of precipitation was recorded in some basins in 1991.

### 2.3. WMA Water Budget

[14] The main source of recharge to the WMA is winter precipitation on the outcrop of the Judea Group. Recharge rates generally range from 25% to 35% of MAP but may range from 20% to 60% of MAP during extreme dry and wet years, respectively [e.g., *Baida and Burstien*, 1970; *Goldshtoff*, 1972b; *Goldshtoff and Ben-Zvi*, 1972; *Baida and Zukerman*, 1992; *Guttman and Zukerman*, 1995b; *Guttman and Zaytun*, 1996].

[15] The mean recharge volume is estimated to be 340–360 $Mm^3\ yr^{-1}$ ($10^6\ m^3\ yr^{-1}$) [*Baida*, 1986]. Minimum recharge was estimated to occur during 1932 (174 $Mm^3\ yr^{-1}$) [*Guttman et al.*, 1988], and maximum recharge occurred during 1991 (800–1200 $Mm^3\ yr^{-1}$) [*Guttman and Zukerman*, 1995a].

[16] Mean annual discharge from the WMA natural outlets prior to groundwater pumpage was 226–228 $Mm^3\ yr^{-1}$ from the Yarqon spring and 91–93 $Mm^3\ yr^{-1}$ from the Taninim spring [*Dafny et al.*, 2008a; *Dafny et al.*, 2008b]. Additional outlets near the Taninim spring add ~6 $Mm^3\ yr^{-1}$ to the discharge. Since the introduction of pumping in the 1930s, groundwater abstraction has gradually increased to ~350–370 $Mm^3\ yr^{-1}$, completely drying the Yarqon spring and reducing discharge from the Taninim spring to 25–30 $Mm^3\ yr^{-1}$ [*Dafny et al.*, 2008b].

### 2.4. Previous Studies

[17] Much work has been conducted attempting to empirically calculate the WMA annual recharge values [*Baida and Burstien*, 1970; *Goldshtoff*, 1972a; *Goldshtoff and Ben-Zvi*, 1972; *Baida and Zukerman*, 1992; *Guttman and Zukerman*, 1995a] (Figure 6). Recharge studies of the WMA progressed through time from the 1970s to the 1990s (as can be seen by the list of references), with the most recent work conducted by *Zukerman* [1999]. *Zukerman* [1999] suggested

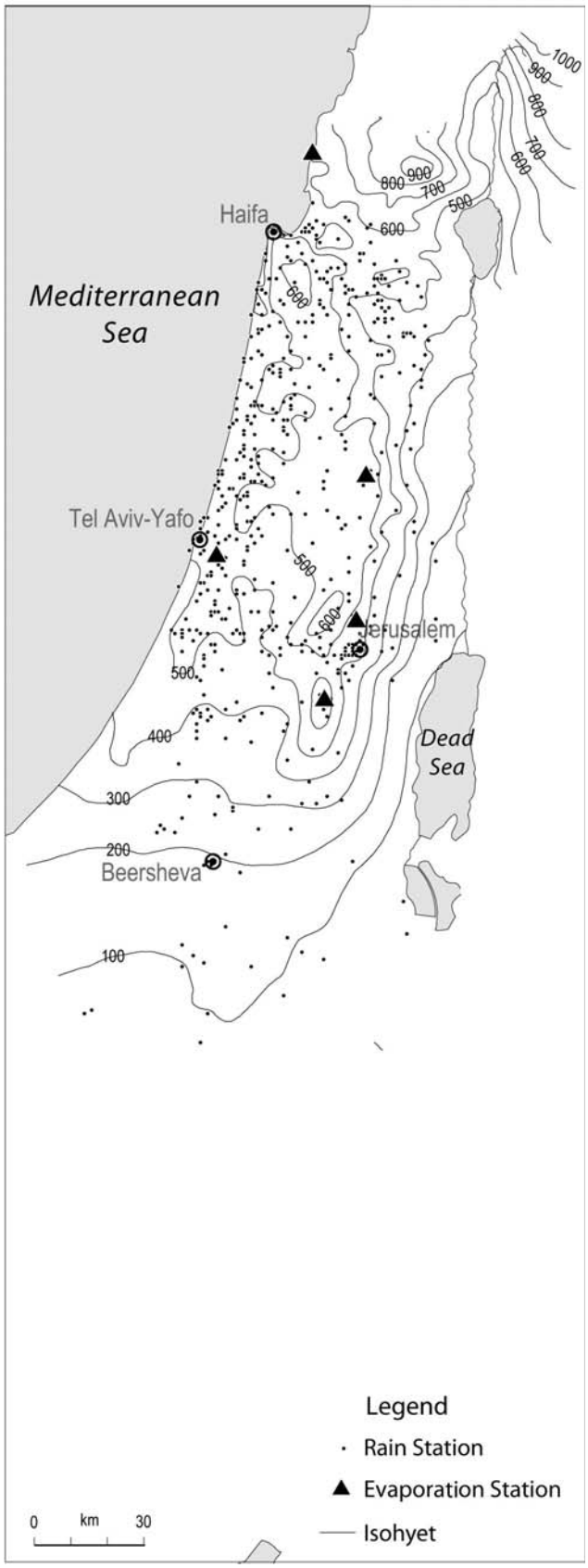


**Figure 5.** A map showing the rain gauge stations used for this study with isohyets of the mean annual precipitation values. Triangles show the pan-A evaporation station locations.

linear relations between the annual recharge (in mm) and annual precipitation ($P$, in mm) for three different scenarios:

$$\text{Recharge} = \begin{cases} 0.45(P-180), & 200\ \text{mm} < P \le 650\ \text{mm} \\ 0.88(P-410), & 650\ \text{mm} < P \le 1000\ \text{mm} \\ 0.97(P-463), & 1000\ \text{mm} < P \end{cases}. \quad (1)$$

The third condition ($P > 1000$ mm) occurred only once over the entire record (the extreme winter of 1991). *Berger* [1999] created a monthly recharge model based on daily precipitation data, artificial recharge (water added for storage in the aquifer through wells), and pumping for the WMA as part of a linked hydrometeorological-hydrogeological model. The hydrogeological output was compared to fluctuations in water table levels and spring discharge. The hydrometeorological model was calibrated on the basis of the previous model results of *Guttman and Zukerman* [1995b], which are reliable on an annual basis but do not provide recharge estimates at high temporal resolution. Although comprehensive, the model does not consider evapotranspiration, which is assumed to be up to 65%–75% of annual precipitation. Recently, *Hughes et al.* [2008] used an uncalibrated distributed model for the WMA, which results in long-term mean recharge of 430 $Mm^3\ yr^{-1}$, which is an overestimate of 23% relative to empirical long-term mean estimates of 350 $Mm^3\ yr^{-1}$. This overestimation is attributed to a bias in calculating mean values over the 1990–1997 period, which includes the exceptional values for 1991. Recharge during 1991 is estimated to be two to three times the long-term mean as a result of extremely high precipitation values that year (twice the long-term MAP).

## 3. Daily Recharge Assessment Model (DREAM)

### 3.1. Model Description

[18] DREAM is based on a daily water budget [*Georgakakos*, 2002] and includes calculation of all water cycle components for a triangular element mesh in the studied basin. The water balance is developed for the vadose zone. Each mesh element has a soil type index $n$ ($n$ = 1 for terra rossa, $n$ = 2 for rendzina, and $n$ = 3 for desert soil) and lithology type index $m$ ($m$ = 1 for limestone/dolomite and $m$ = 2 for chalk/marl). Each mesh element is a modeling unit for which the water budget is applied:

$$Z_n\theta(t+1,i) = Z_n\theta(t,i) + \text{RA}(t,i) - \text{ET}(t,i) - \text{RE}(t,i) - \text{RU}(t,i), \quad (2)$$

where RA is daily precipitation (millimeters), ET is daily evapotranspiration (in mm), RE is daily recharge (in mm), RU is daily runoff (in mm), $Z_n$ is effective soil thickness (in mm) according to soil type $n$, $\theta$ is water content (fraction), $t$ is time (days), and $i$ is mesh element index (1,…, 3364). Output at the base of the vadose zone constitutes RE. The different lithologies of the elements are manifested in RE as shown in equations (3) and (10).

[19] The modeling unit can be conceptualized as a tank with one inlet and three outlets at different elevations representing activation of different output contributions as a function of soil moisture content (Figure 7). The inlet

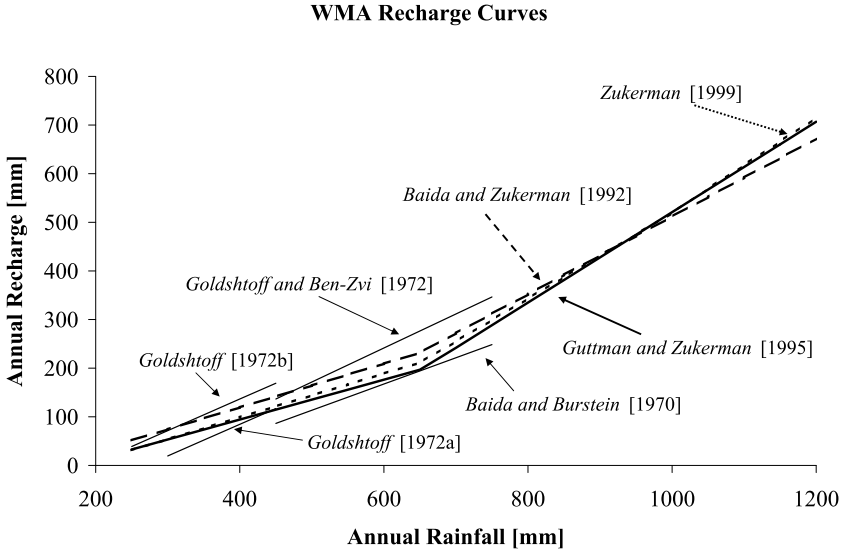


**Figure 6.** Previous studies of the WMA, showing the different recharge curves produced.

represents daily precipitation over the area (RA). The three outlets represent the following.

[20] 1. ET, which produces output only when the water content in the tank is higher than the soil permanent wilting point, $\theta_n^{\mathrm{pwp}}$. This is expressed by

$$\mathrm{ET}(t,i) = Z_n \theta(t,i) \beta. \tag{3}$$

[21] 2. RE, which produces output only when the water content in the tank exceeds soil field capacity, $\theta_n^{\mathrm{fc}}$. This is expressed by

$$\mathrm{RE}(t,i) = Z_n \theta(t,i) \mu_m. \tag{4}$$

[22] 3. RU, which produces output only when the water content in the tank reaches saturation (porosity), $\theta_n^s$. This is expressed by

$$\mathrm{RU}(t,i) = \mathrm{RA}(t,i) - Z_n \theta_n^s(t,i). \tag{5}$$

[23] Accordingly, the computation is done in three steps (represented by an indexing to $\theta$ $(t,i)$ in the following equations):

[24] 1. The soil water content is increased by the daily precipitation divided by the soil effective thickness, where water in excess of saturation becomes runoff:

$$\theta^1(t,i) = \left\{ \begin{array}{cc} \theta(t,i) + \mathrm{RA}(t,i)/Z_n, & \theta(t,i) + \mathrm{RA}(t,i)/Z_n > \theta_n^s \\ \theta_n^s, & \theta(t,i) + \mathrm{RA}(t,i)/Z_n \geq \theta_n^s \end{array} \right\} \tag{6}$$

$$\mathrm{RU}(t,i) = \left\{ \begin{array}{cc} 0, & \theta(t,i) + \mathrm{RA}(t,i)/Z_n < \theta_n^s \\ \mathrm{RA}(t,i) - Z_n(\theta_n^s - \theta(t,i)), & \theta(t,i) + \mathrm{RA}(t,i)/Z_n \geq \theta_n^s \end{array} \right\}. \tag{7}$$

[25] 2. If soil water content exceeds the soil permanent wilting point, daily ET occurs. Potential evapotranspiration (PET) is computed from daily panevaporation data, Pan(t,i) (millimeters) interpolated from observations (see section 3.2, Figure 5), multiplied by a PET factor $\beta$ representing transformation from panevaporation to PET from a unit of soil covered by vegetation. The $\beta$ parameter is assumed to be uniform all over the WMA recharge area. Actual ET values are computed from PET and soil water content [*Dingman*, 1994]:

$$\mathrm{ET}(t,i) = \left\{ \begin{array}{cc} 0, & \theta_n^{\mathrm{pwp}} > \theta^1(t,i) \\ \beta\,\mathrm{Pan}(t,i)\left(\dfrac{\theta^1(t,i) - \theta_n^{pwp}}{\theta_n^{fc} - \theta_n^{pwp}}\right), & \theta_n^{\mathrm{pwp}} \leq \theta^1(t,i) < \theta_n^{\mathrm{fc}} \\ \beta\,\mathrm{Pan}(t,i), & \theta^1(t,i) \geq \theta_n^{\mathrm{fc}} \end{array} \right\} \tag{8}$$

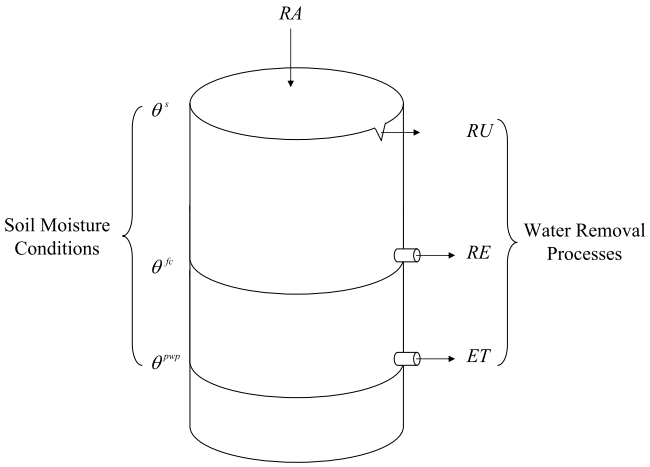


**Figure 7.** The conceptual model of DREAM. A tank with one inlet for precipitation (RA) and three outputs. The bottom outlet for evapotranspiration (ET) produces output only when the water level in the tank is above the permanent wilting point, $\theta^{\mathrm{pwp}}$. The second outlet for recharge (RE) produces output only when the water level in the tank is above field capacity, $\theta^{\mathrm{fc}}$. The top outlet produces runoff (RU) when the water content in the tank reaches saturation (porosity,$\theta^s$).

**Table 1.** Soil Moisture Content Values[a]

| | Terra Rossa ($\theta_1$) | Rendzina ($\theta_2$) | Desert Soil ($\theta_3$) |
|---|---|---|---|
| $\theta^s$ | 0.46 | 0.46 | 0.45 |
| $\theta^{fc}$ | 0.32 | 0.30 | 0.25 |
| $\theta^{pwp}$ | 0.17 | 0.15 | 0.10 |

[a]From data by *Dingman* [1994].

$$\theta^2(t,i) = \theta^1(t,i) - \mathrm{ET}(t,i)/Z_n. \quad (9)$$

When $\theta(\mathrm{t,i}) < \theta_n^{fc}$, plants are considered to be water-stressed, whereas when $\theta(\mathrm{t,i}) = \theta_n^{fc}$ (the bracketed expression in equation (8) becomes 1), plants are considered to be unstressed [*Dingman*, 1994].

[26] 3. Daily recharge (RE) occurs when water content in the tank exceeds soil field capacity. Recharge is calculated as a fraction of the water in the soil using a recharge factor, $\mu_m$ that depends on lithological type $m$:

$$\mathrm{RE}(t,i) = \begin{Bmatrix} 0, & \theta_n^{fc} > \theta^2(t,i) \\ Z_n\theta^2(t,i)\mu_m, & \theta_n^{fc} \le \theta^2(t,i) \end{Bmatrix} \quad (10)$$

$$\theta^3(t,i) = \theta^2(t,i) - \mathrm{RE}(t,i)/Z_n. \quad (11)$$

[27] Finally, soil water content at the end of this process is the initial soil water content for the following day:

$$\theta(t+1,i) = \theta^3(t,i). \quad (12)$$

This procedure is carried out continuously for the entire period analyzed. The computation is done for each of the 3364 mesh elements, each having specific daily precipitation and evaporation data, as well as for specific lithology and soil types.

[28] DREAM was designed to include a limited number of model parameters for robustness and to reduce uncertainties related to parameter calibration. The soil water content variables ($\theta_n^s$, $\theta_n^{fc}$, and $\theta_n^{pwp}$) were obtained from the literature (Table 1) [*Dingman*, 1994]. The six model parameters requiring calibration are three soil effective thickness parameters ($Z_{1-3}$), two lithology recharge factor parameters ($\mu_{1,2}$) and a pancoefficient parameter ($\beta$). The calibrated parameter values dictate the size of the different tanks and outlet openings.

### 3.2. Precipitation, Evaporation, and Surface Data of the WMA

[29] The WMA recharge area was divided into 3364 mesh elements (mean area of 0.6 km$^2$) in accordance with the linked groundwater flow model (FEFLOW; see section 3.3).

[30] The two most significant inputs into the DREAM are daily precipitation and panevaporation. Precipitation data were assembled using all available daily rain gauges within a 15 km buffer around the WMA recharge zone (Figure 5). A smaller buffer (2 km) was used for gauges east of the recharge zone because of abrupt changes in precipitation beyond the main water divide caused by the rain shadow of the Samaria Hills. The number of operating rain gauges varies from year to year and within a year, with a mean of 350 active gauges per day (234–430 gauges on a given day). Daily precipitation data were interpolated to the 3364 mesh elements. The interpolation chosen was of an inverse distance weighting method to a power of 2, which was found to be superior to other local weighted regressions [*Kurtzman et al.*, 2009].

[31] Daily panevaporation data for each of the 3364 mesh elements were created in the same manner using data from seven daily evaporation pan-A stations (Figure 5). Pedology and lithology for each mesh element were defined using geographic information system coverage. Soil and rock types were assigned to each element according to the dominant type found in each element.

### 3.3. Groundwater Flow Model

[32] DREAM was linked to a numerical groundwater flow model for the WMA that was built using the FEFLOW software of DHI-WASY [*Dafny et al.*, 2008b]. It follows the hydrogeological concepts (water budget, heads, and boundaries) that were designed for the WMA conceptual model [*Dafny et al.*, 2008a]. The model solves mass balance and continuity equations for groundwater flow in saturated porous media. The model grid comprises approximately 7000 triangular finite elements, of which 3364 are in the recharge zone. Daily recharge data computed by DREAM were accumulated to monthly values and used as input to the linked groundwater flow model (FEFLOW).

## 4. Model Application

### 4.1. Calibration

[33] The calibration period was 1987–2002. The model was calibrated in three stages. The first stage was to comply with the historical preexploitation mean annual spring discharge values. The second stage was to comply with the FEFLOW quasi-static calibration for the same period (preexploitation), producing adequate spatially distributed values. The third stage was to comply with the FEFLOW transient calibration.

[34] For the first and second calibration stages that were aimed at fitting annual mean recharge values, inclusion of the extremely high precipitation year of 1991 in the 17 year calibration record would bias the estimated model parameter values, and therefore the data from the 1991 year were omitted from these two stages. This year was included, however, in the transient stage calibration.

#### 4.1.1. First Stage

[35] The first calibration stage was aimed at fitting the natural mean annual discharge values of the two aquifer outlets, Yarqon and Taninim springs, before pumping was introduced. The target values of 97–99 Mm$^3$ yr$^{-1}$ for the Taninim spring (Carmel and Samaria subbasins) and 226–228 Mm$^3$ yr$^{-1}$ for the Yarqon spring (Benjamin, Jerusalem, Judea, and Negev subbasins) were obtained from historical spring discharge data (preexploitation values: 1930s).

[36] Approximately $10^6$ model runs were conducted to calibrate the six parameters ($Z_{1-3}$, $\mu_{1,2}$, and $\beta$). The calibration process assigned sets of values to the elements according to the element parameters. Each element has designated thickness ($Z$), recharge coefficient ($\mu$), and pancoefficient ($\beta$) values in accordance with the pedology and lithology of the element. This procedure assigns the same $Z_1$

**Table 2.** Calibration Value Results

| $Z_{1-3}$ (mm) | $\mu_{1,2}$ | $\beta$ |
|---|---|---|
| 800 | 0.0165 | 0.95 |
| 1400 | 0.0140 | |
| 150 | | |

value for all elements covered by terra rossa soil, the same $Z_2$ value for all elements covered by rendzina soil, and so on. The spatial variability was derived from the spatial variability of the soil types and the lithological variability. The calibration values varied for $Z_{1-3}$ from 50 to 3000 mm; they varied for $\mu_{1,2}$ from 0.0001 to 0.02; and they varied for $\beta$ from 0.5 to 1. For each run, the mean annual recharge at each of the two springs was computed and compared to the reference values above using two objective functions: the relative root-mean-square error (RRMSE, defined as the root-mean-square error divided by the mean observed value) and the multiplicative relative Bias (RBias, defined as the ratio between average computed to average observed value). The model runs with an RBias of 0.9–1.1 and an RRMSE value of <0.05 were selected for further analysis, which consisted of 1% of the $10^6$ original runs. Additional constraints were introduced to eliminate runs with unreasonable values for ET, RU, and RE (such as zero annual ET, etc.), resulting in ~50 acceptable parameter sets.

#### 4.1.2. Second Stage

[37] Recharge output from DREAM with acceptable parameter sets were run through the FEFLOW model. The data used were for a single average year, which was run repeatedly to assess stability of groundwater levels (quasi-static calibration). Each parameter set was evaluated for the preexploitation time for the FEFLOW model according to the six recharge areas. More parameter sets were eliminated by removing all sets that produced unstable groundwater levels relative to representative summer groundwater levels. Model stability was assessed by examining groundwater levels in all six zones exhibiting either stable values (rising in the winter and returning to original levels in summer) or continuously rising/falling groundwater levels. In addition, at this stage, fine tuning of hydraulic conductivity and spring coefficients of the FEFLOW model was conducted.

#### 4.1.3. Third Stage

[38] This calibration stage involved the group of solutions deemed reasonable from the second stage. These results were all run using FEFLOW for transient calibration, allowing tuning of storativity parameters. The run consisted of the entire set of daily values (accumulated to monthly) for the duration of the calibration period. Out of all available solutions the parameter set that produced the best fit to measured groundwater levels was chosen as the optimal result for DREAM (Table 2). Quantitative methods for choosing the optimum result at this stage are presented by *Dafny et al.* [2008b] as a part of the FEFLOW calibration process. After cocalibrating the DREAM and FEFLOW models, recharge values could be calculated and then used to simulate groundwater levels.

[39] The linked results agree well with measured groundwater table fluctuations. An example of the water table fluctuation is presented in Figure 8. *Dafny et al.*

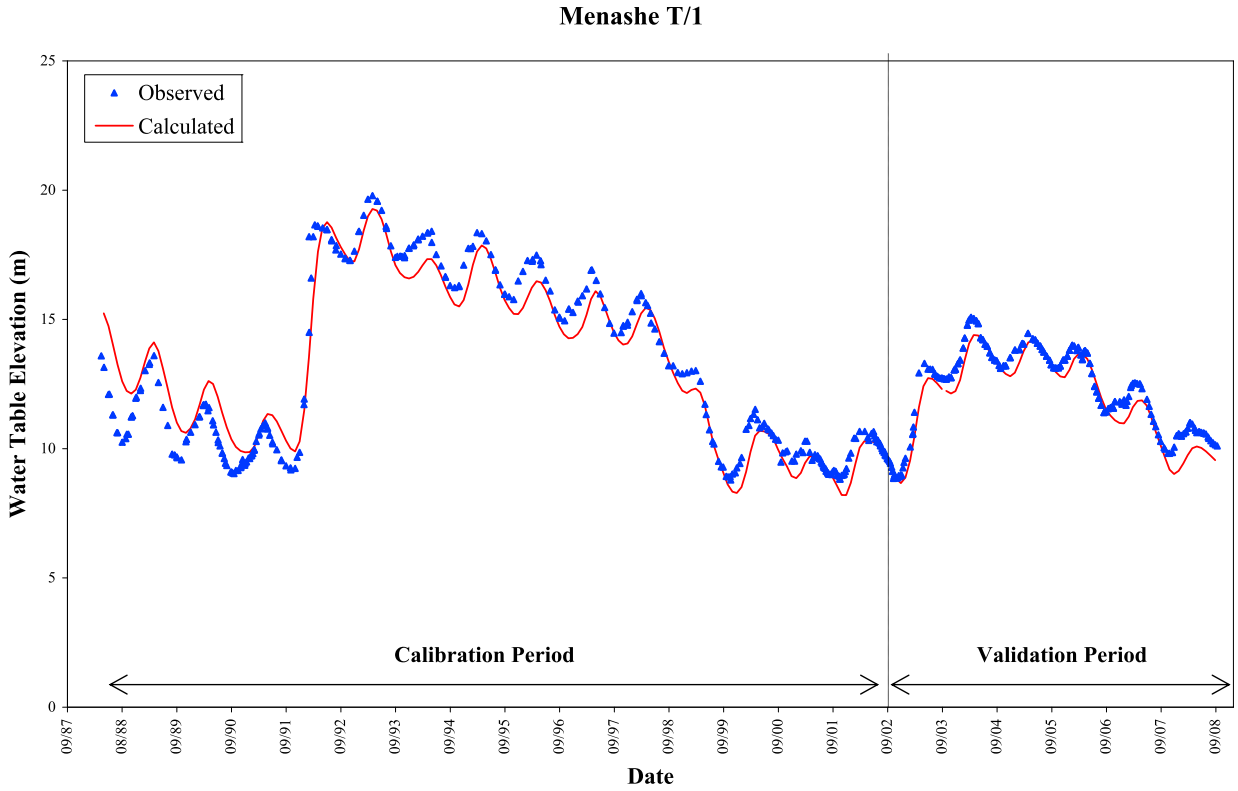


**Figure 8.** Observed and calculated water table fluctuations at the Menashe T/1 well. The observed data are given with monthly resolution. The slight deviation at the beginning is due to the initial conditions of the model, which are nulled within a single year.

[2008b] present a comprehensive description of the linked water table fluctuation calculations in many wells in the WMA.

### 4.2. Model Validation

[40] DREAM was validated for 2002–2007 by (1) comparing annual recharge values for the validation and calibration periods (checking for extreme deviations) and (2) using DREAM recharge results as input to the FEFLOW model and comparing measured and simulated water table fluctuations. Computed annual recharge agrees well with the precipitation-recharge calibration values of DREAM for previous years both for the entire WMA (Figure 9a) and for each separate subbasin (Figure 9b). Validation results also provide a good fit between simulated and measured groundwater levels ($R^2 = 0.95$; RRMSE = 4.8%; RBias = 1.04) when DREAM results are combined with the FEFLOW model (Figure 8). Furthermore, both normal and extreme years (rainy years and droughts) in the calibration period (such as 1991 and 1998, respectively) are well simulated, as are those in the validation period (the rainy 2002 year and the five successive droughts that followed).

## 5. Precipitation–Recharge Relationships

### 5.1. Recharge Evaluation for WMA Record

[41] Although problematic, the recharge results from DREAM were compared to a recharge model based on annual data because such annually based models provide the only prior recharge estimates for reference.

[42] Annual recharge varied from 21 to 442 mm, representing 9%–40% of annual precipitation. The main factor controlling annual recharge is annual precipitation ($R = 0.71$). Additional variability in simulated recharge for similar precipitation values is attributed to varying spatial and temporal distribution of precipitation that affects recharge. Annual recharge rates from DREAM generally agree with previous recharge results from the WMA. The relationship between annual recharge and precipitation described by equation (1) from *Zukerman* [1999] is shown for comparison in Figure 9 (dotted line). Because it is based on annual precipitation, it is obviously limited to a single estimation result for each annual precipitation value, whereas DREAM allows a variety of recharge results for the same annual precipitation according to daily precipitation patterns. The primary difference between the recharge relationship of *Zukerman* [1999] and DREAM recharge estimates is in the extreme values for 1991, where the former study results in 542 mm recharge (~50% of precipitation for that year), whereas DREAM estimates 442 mm (40% of precipitation for that year). DREAM accounts for ET and produces RU estimates as well as recharge estimates. During 1991, the measured RU by the IHS rose to 8%–12% of precipitation for that extreme winter (as opposed to 3%–5% for average years). DREAM estimates similar RU values for 1991. Use of the *Zukerman* [1999] relationship reduces estimated ET values to $\leq$40%, which are extremely low values. Furthermore, using measured pan-A evaporation data in DREAM provides a more complete water budget calculation including all components. The partial water budget by *Zukerman* [1999] might not be as reliable.

[43] Computed annual recharge for each of the six recharge zones shows three distinct recharge regimes (Figure 9b). The first includes recharge for $\leq$400 mm annual precipitation (either in dry years or in dry regions, such as the Negev desert); the second includes recharge from 400 to 1000 mm annual precipitation; and the third regime is for $\geq$1000 mm of precipitation (1991). These three regimes slightly resemble the three regimes in equation (1) [*Zukerman*, 1999], where the first break is at 650 mm and the second at 1000 mm. In this study the disaggregation into six subbasins allows examination of dry values (with two subbasins in desert areas, Negev and Judea), whereas in equation (1) recharge calculation was for annual precipitation averaged for the entire aquifer recharge area.

[44] Differences between results from *Zukerman* [1999] and this study in terms of recharge as a percentage of precipitation are marked in very wet years (Figure 9c). Recharge increases significantly as a percentage of annual precipitation in Zukerman's work, whereas results from DREAM show that recharge reaches a maximum percentage of annual precipitation and levels off. This result is related to increased runoff during wet years (such as 1991) (Figure 9c).

[45] Similarity in recharge results between DREAM and those based on annual data provides initial confidence in recharge results from DREAM, and the large variability found points to the importance of a temporally distributed model rather than an annually based model. Furthermore, Zukerman's relationship can only be used in retrospect. Only after the annual precipitation value is known can recharge be evaluated, whereas with DREAM, recharge can be estimated in near real time.

### 5.2. Sensitivity Analysis

[46] Local sensitivity analysis was conducted to assess the relative importance of several factors to recharge: precipitation, panevaporation, soil moisture parameters ($\theta_n^s$, $\theta_n^{fc}$, and $\theta_n^{pwp}$), and model parameters ($Z$, $\mu$, $\beta$). Values for each factor were varied separately within ±20% for the entire recharge area over the modeled period, and the resultant change in total recharge volume was computed (Table 3). The model is most sensitive to precipitation amount, with a 31% change in recharge for a 20% change in precipitation. The model is also very sensitive to field capacity. This value sets the threshold for recharge occurring. A higher value for $\theta_n^{fc}$ raises this threshold, keeping water from recharging the aquifer and forcing ET to remove a larger portion of soil moisture. The remaining factors resulted in $\leq$20% variation in recharge.

## 6. Effect of Temporal Precipitation Patterns

### 6.1. Natural Observations

[47] Similar amounts of annual precipitation yield significantly different amounts of recharge (Table 4). This difference between annual precipitation and recharge is attributed to intraseasonal variability in precipitation as a result of temporal distribution of precipitation during the wet winter season. Although approximately the same amount of precipitation occurred during 1993 (400 mm) and 1999 (414 mm), 80% of the precipitation fell during 4 months in 1993 (mid-November to mid-March) and during two months in 1999 (January and February) (Figure 10 and

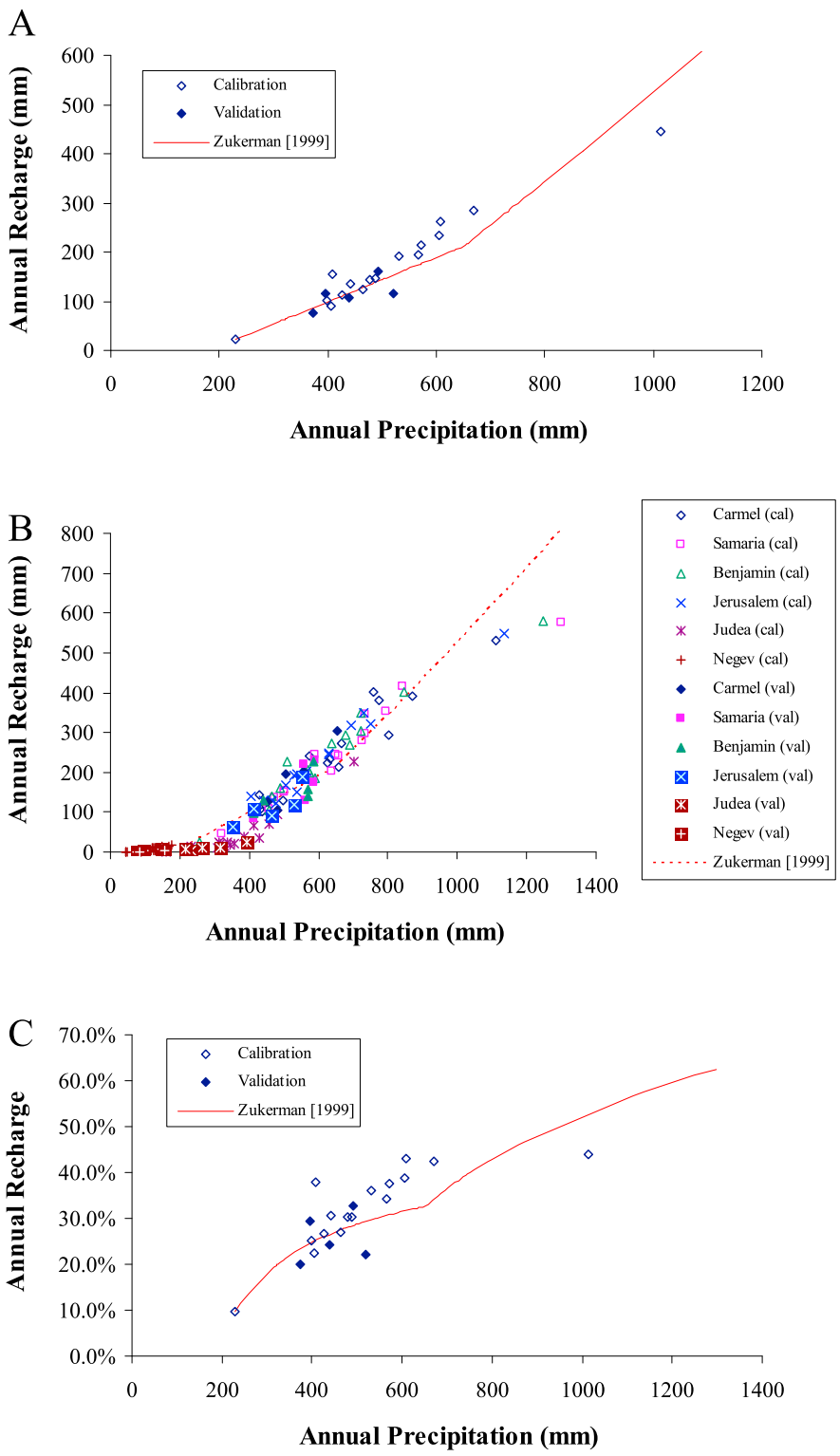


**Figure 9.** Recharge evaluation results. The open symbols are for the calibration period, and the solid points are for the validation period. In all cases, the validation values fit well within the calibration values (i.e., they do not deviate much from the average). (a) The annual recharge values (in mm) in relation to the annual precipitation values (in mm) for the whole WMA. The results highly resemble the recharge curve of *Zukerman* [1999]. (b) The annual recharge values (in mm) for each of the six subbasins in relation to the annual precipitation values (in mm). The main deviation found between this study and that of *Zukerman* [1999] is in the high values (>1000 mm). Calibration results (open symbols marked "cal") and validation results (solid symbols marked "val") are shown. (c) The annual recharge percentage for each part of the whole WMA. The results in this study show leveling out of the recharge percentage, whereas in the work of *Zukerman* [1999], the recharge percentage keeps rising up to over 50%.

**Table 3.** Local Sensitivity Analysis[a]

| | Maximum Resulting Change (%) |
|---|---|
| Precipitation | ±31 |
| $\theta^{fc}$ | ±21 |
| $Z$ | ±16 |
| $\beta$ | ±12 |
| Pan | ±12 |
| $\mu$ | ±9 |
| $\theta^{s}$ | ±4 |
| $\theta^{pwp}$ | ±3 |

[a]Shown is the change in total recharge volume resulting from a local change of ±20% in the examined factors.

Table 4, set 1). The temporal precipitation distribution during 1993 did not result in soil moisture exceeding field capacity, whereas the short rainy season during 1999 increased and maintained soil moisture above field capacity during most of this time (Figure 10). The temporal distribution caused the same effect for sets 2 and 3 (Table 4). The 10% (of precipitation) at the beginning and ending of the season were omitted because of different synoptic influences

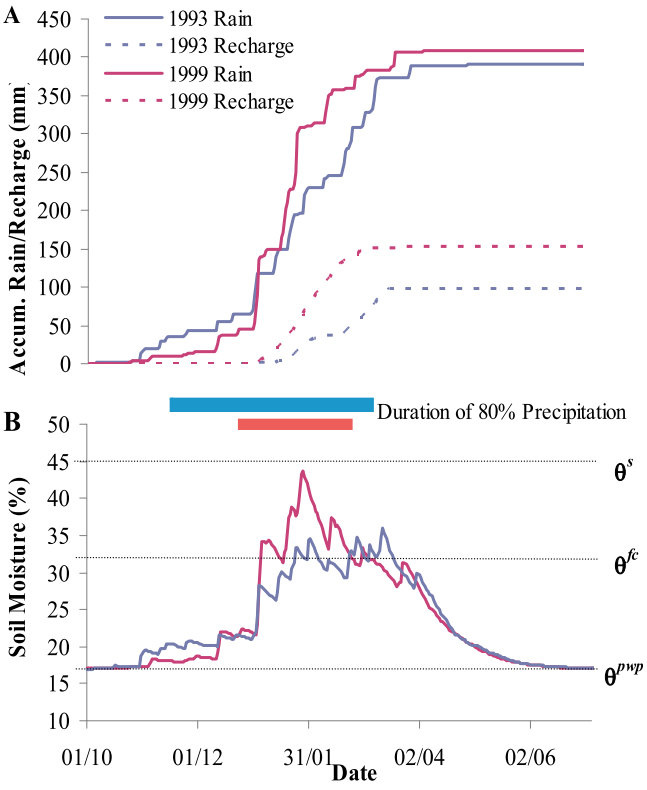


**Figure 10.** A comparison of precipitation-recharge relationships for 2 years with a similar amount of precipitation, 1993 (400 mm) and 1999 (414 mm). (a) Accumulated precipitation and recharge and (b) soil moisture content. In 1999, 80% of the precipitation fell during 2 months, whereas the same fraction fell in 1993 over a period of 4 months. The temporal precipitation distribution during 1993 did not allow the soil water content to rise much above the field capacity values, whereas during 1999, the short rainy season increased and held the soil water content high above field capacity to allow for recharge to occur for most of this period and with high rates.

**Table 4.** Recharge Variability Results for Similar Precipitation Values

| Year | Precipitation (mm) | Recharge (mm) | Recharge Percentage |
|---|---|---|---|
| | | *Set 1* | |
| 1999 | 414 | 155 | 37 |
| 1993 | 400 | 99 | 25 |
| | | *Set 2* | |
| 1992 | 570 | 213 | 37 |
| 2001 | 569 | 195 | 34 |
| | | *Set 3* | |
| 1987 | 610 | 260 | 43 |
| 1994 | 612 | 235 | 39 |

involved during the autumn and spring seasons, whose precipitation mainly falls in the southern parts of Israel and contributes very little to the WMA [*Goldreich*, 1998].

[48] To better understand the influence of temporal precipitation patterns on recharge, a similar analysis was conducted on a smaller area. When comparing years with similar amounts of precipitation in a single subbasin, it is apparent that the temporal distribution of precipitation plays an important role. In some cases, years with high values of

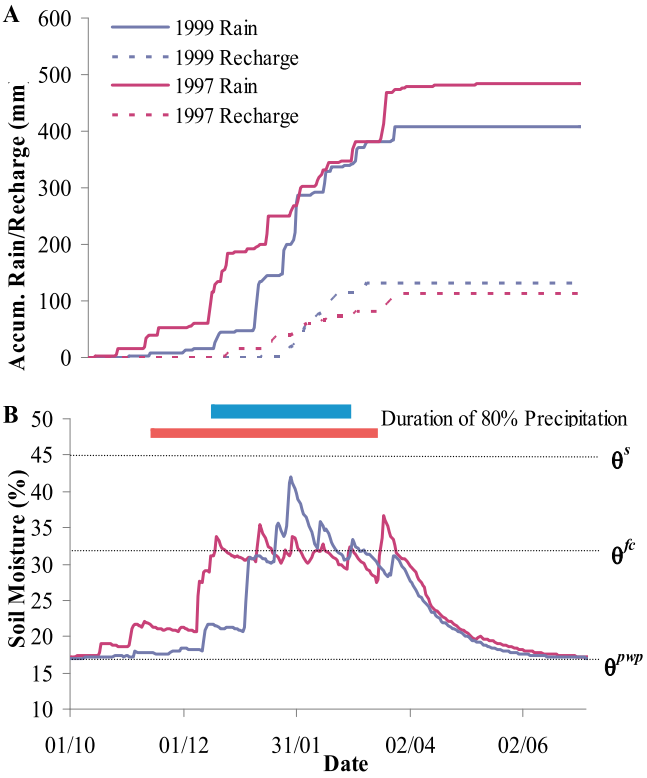


**Figure 11.** A comparison of precipitation-recharge relationships for 2 years with a similar amount of precipitation, 1997 (485 mm) and 1999 (414 mm), for a single subbasin (Benjamin). (a) Accumulated precipitation and recharge and (b) soil moisture content. In 1999, 80% of the precipitation fell during 2.5 months, whereas the same fraction fell in 1997 over a period of more than 4 months. The amount of precipitation during 1997 is higher than that during 1999, but the recharge is actually lower.

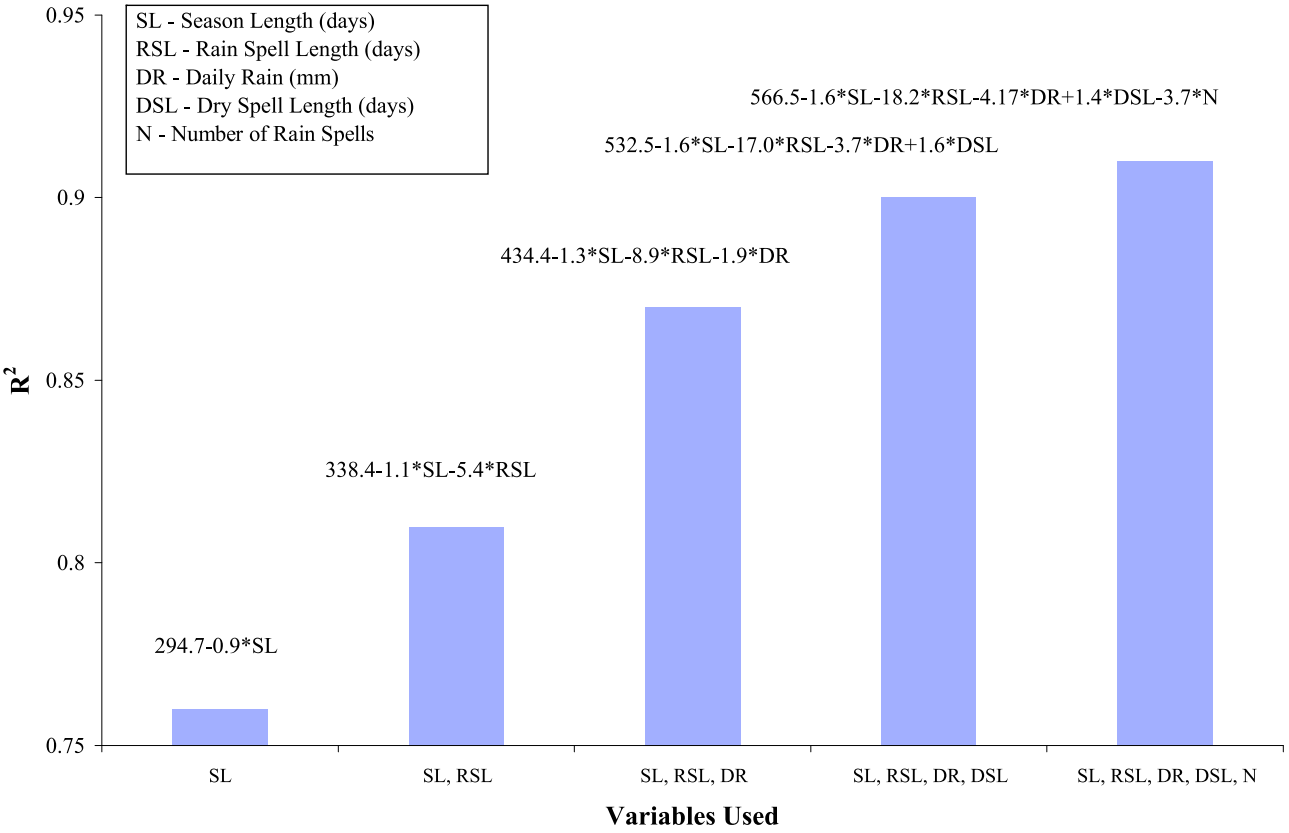


**Figure 12.** A graph showing the increase in ability to explain the recharge variability for a known value of annual precipitation (600 mm). Multivariant regressions were conducted with one to five different factors in the precipitation temporal distribution. For each number of independent variables, the combination that best explains recharge variability is shown. The graph shows the rise in goodness of fit (from 0.76 for a single factor to 0.91 for all five factors). The regression expression is shown for each case.

annual precipitation produce less recharge than years with less precipitation (Figure 11). Comparison of cumulative precipitation and recharge between 1997 (485 mm) and 1999 (414 mm) for a single subbasin (Benjamin) shows that although precipitation was much greater during 1997, recharge was less during 1997 (114 mm, 24% of precipitation) than in 1999 (131 mm, 32% of precipitation). The difference in recharge rates is attributed to the length of the rainy season: 80% of precipitation fell during 4 months in 1997 versus 2.5 months in 1999. The two examples discussed above suggest that the main factors governing daily soil moisture content and consequently recharge are dry spells and rainy season length. Dry spells during the rainy season allow water to be removed by ET, reducing available water for recharge and occasionally reducing soil moisture content below field capacity. Extending the rainy season dictates this recharge reduction by either adding more dry spells or having longer dry spells during the rainy season. In summary, for a given amount of precipitation, the longer the rainy season, the less effective it is for recharge.

### 6.2. Synthetic Simulations

[49] To further investigate the effect of temporal precipitation distribution, a synthetic data set was created for DREAM. This data set was designed to focus on precipitation patterns within the year and eliminate any other source of variability, including variability in annual precipitation amount and spatial variability in precipitation. The simulation was conducted for 87 years with mean annual precipitation of 600 mm uniformly distributed over the recharge zone. The differences introduced were as follows: season length (SL; 35–220 days); length of precipitation period (rainy-spell length; RSL; 3–13 days); daily precipitation values (DR; 12–40 mm); length of dry periods (dry-spell length: DSL; 10–60 days); and number of wet/dry periods ($N$; 2–10). Potential evaporation data used in these simulations were the climatological evaporation data (long-term mean evaporation values) [*Goldreich*, 1998] for non-rainy days and 50% of the climatological evaporation for rainy days. The statistics were focused on a single subbasin as conducted with the natural data to eliminate spatial variability of the different climatic zones in Israel (arid, semi-arid, and Mediterranean climates). The simulated annual recharge rates from DREAM ranged from 55 to 250 mm (mean 184 mm), indicating that up to 106% of the difference in recharge can be potentially attributed to factors that are solely related to temporal patterns in precipitation.

[50] To identify the most important factors related to temporal precipitation pattern affecting annual recharge rates, a multiple linear regression analysis was conducted for the 87 years of data (Figure 12) with the five variables considered as independent variables (SL, RSL, DR, DSL, and $N$) and DREAM-simulated recharge rates as the

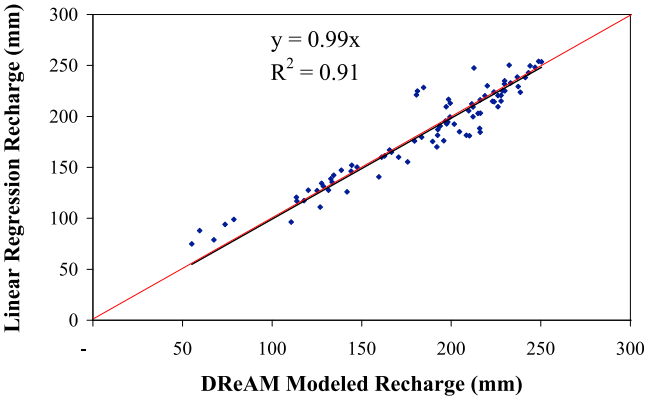


**Figure 13.** A graph showing the ability to predict the recharge in the Benjamin subbasin for a known precipitation value, according to the temporal variability. The horizontal axis presents annual recharge values calculated using DREAM from the synthetic daily data. The vertical axis presents recharge values calculated using the multiple linear regression presented in Figure 12.

dependent variable. As a single factor, the season length was found to be the dominant factor, explaining 76% of recharge variability in the synthetic data set. All other factors considered explain less than 23% of recharge variability in this framework. Considering two explanatory factors, season length and length of precipitation provide the highest explained variability of 80%, although the combination of season length with either number of wet/dry periods or length of dry periods gave similar results. The combination of three factors (season length, length of precipitation, and daily precipitation value) explained 87% of the variability, while the combination of four factors (season length, length of precipitation, daily precipitation value, and length of dry periods) explained 90% of recharge variability. Using all factors explained 91% of recharge variability (Figure 12). Using a multiple linear regression (Figure 12), we predicted the recharge for the Benjamin basin:

$$\mathrm{RE} = 566.5 - 1.6\mathrm{SL} - 18.2\mathrm{RSL} - 4.17\mathrm{DR} + 1.4\mathrm{DSL} - 3.7N. \quad (13)$$

Good agreement between the two recharge estimation methods was found ($R^2$ = 0.91; Figure 13).

## 7. Discussion

[51] DREAM is a precipitation-recharge model that links to hydrogeological groundwater flow models. It can be applied in different regions and at variable spatial scales [*Sheffer*, 2009]. Application of DREAM for the WMA is presented in this work.

[52] Although annual precipitation is highly correlated with annual recharge ($R^2 \geq 0.7$ in many studies), relating recharge to precipitation at a higher temporal resolution is more of a challenge. To relate precipitation to recharge at a high temporal scale, models have to be introduced that take into account changes in soil moisture, which plays an important role in the high temporal recharge process. *Gregory* [2006] and *Wilcox et al.* [2008] measured direct recharge in a cave, showing the response of the cave to each precipitation event, with a high correlation on an annual basis. When they tried to relate single recharge responses to precipitation events the correlation was poor. *Sheffer et al.* [2008] conducted a similar study in a cave subjected to a Mediterranean climate, showing that although an event-based correlation yields poor results, consideration of soil moisture improves understanding of the recharge process tremendously. Recharge occurred in response to soil moisture conditions prior to the precipitation. In the case of dry soil, even an extreme precipitation event did not result in a recharge response in the cave, whereas other precipitation events yielded high recharge when the soil had sufficient initial moisture [*Sheffer et al.*, 2008].

[53] In recent years, observed climate trends suggest shifts in precipitation regime in the eastern Mediterranean. Although the overall annual precipitation has not changed significantly, some studies point to a positive trend in heavy precipitation and a negative trend in light precipitation [e.g., *Alpert et al.*, 2002]. This type of change causes precipitation to fall as isolated events. In the past, winters had moderate precipitation events lasting 2 to 3 days every week to 10 days [*Goldreich*, 1998], whereas current and possibly future climate, if indeed the change suggested above occurs, will result in extreme precipitation events followed by long dry spells. On the basis of the results of this study, this transformation in precipitation regime should reduce groundwater recharge.

[54] Short, intense precipitation events cause a rapid increase in soil moisture, which could lead to loss of water by means of runoff. Long dry spells after a precipitation event lead to further loss of soil moisture through ET, leaving a much smaller fraction of the overall precipitation for aquifer recharge. This behavior is manifested in 2007, which was declared a drought year, with less than 70% of MAP in most of Israel [*Israel Hydrological Service*, (*IHS*), 2008]. The low amount of precipitation distributed over a long season (November–May) caused an extreme reduction in groundwater levels below the declared Red Lines, which are the lower limits for groundwater abstraction. This year was the fourth successive drought in Israel and brought water resources to a 20 year low [*IHS*, 2008]. A fifth drought year could result in the lowest values for water resources on record, reaching the Black Lines, which are water table levels so low that irreversible damage might be inflicted on water resources.

## 8. Conclusions

[55] A daily recharge assessment model (DREAM) based on daily water budget calculations of precipitation and evaporation was developed. Linkage of this model to FEFLOW proved an extremely useful approach for simulating recharge in Mediterranean to semiarid regions. Application of this model to the dynamic Western Mountain Aquifer simulated recharge for calibration and validation periods and improved the spatiotemporal resolution of recharge estimation and the ability to provide potentially near-real-time recharge estimates relative to previous recharge studies that were limited to annual recharge estimations. DREAM was able to simulate extreme years as well as average years both in the calibration and validation periods.

[56] This model allows evaluation of controls on recharge apart from annual precipitation. Applying DREAM to the

WMA revealed that the most important factors controlling recharge to the aquifer are annual precipitation and rainy season length. Normally, increased precipitation results in more recharge. However, this study shows that years with similar annual precipitation may yield different amounts of recharge according to the rain season length. Longer rainy seasons allow more or longer dry spells (for a given precipitation amount), resulting in removal of soil moisture through ET rather than recharge, thus reducing the amounts of water available for recharge. This was observed in recharge assessments in the data and was also apparent in the 87 years of synthetic experiment data used. This issue could not be addressed by previous approaches applied to this region that were limited to annual recharge estimations. Furthermore, this links to a possible change in recharge regime resulting from climate change. Intense isolated precipitation events followed by long dry periods may cause a decrease in available water for aquifer recharge even if the total annual precipitation value is sustained or even increases.

[57] Finally, the near-real-time recharge estimation ability of DREAM is a valuable tool for assessing impacts of climate variability at high temporal and spatial resolution and for improved management of water resources.

[58] **Acknowledgments.** This work was funded by the Israel Water Authority. Rain gauge data were obtained from the Israel Meteorological Service and hydrological data from the Israel Hydrological Service. The authors wish to thank the anonymous reviewers for their important comments for the improvement of the manuscript. The authors also wish to thank Bridget Scanlon for editing the manuscript, Shlomo Zlouf and the entire computer team at the Hebrew University of Jerusalem for assistance in parallel computing calibration, Tamar Soffer for map production, Adi Ben-nun for GIS assistance, and Tamir Grodek for fruitful discussion.

## References

Abbott, P. L. (1975), Hydrology of Edwards limestone, south-central Texas, *J. Hydrol.*, *24*(3–4), 251–269, doi:10.1016/0022-1694(75)90084-0.

Alpert, P., et al. (2002), The paradoxical increase of Mediterranean extreme daily rainfall in spite of decrease in total values, *Geophys. Res. Lett.*, *29*(11), 1536, doi:10.1029/2001GL013554.

Arkin, Y. (1967), Explanations to geological map of Jerusalem-Bet Shemesh area, *Isr. J. Earth Sci.*, *16*(1), 46–47.

Baida, A. (1986), The Yarqon-Taninim Aquifer: Quantitative and qualitative aspects in the current water budget of Israel, *EYAL Negev Cent. Res. Dev.*, *86*(6), 51–57.

Baida, A., and Burstien (1970), Recharge to the Y-T basin, Tahal Consult. Eng., Tel Aviv, Israel.

Baida, A., and H. Zukerman (1992), The exploitation and development potential of groundwater resources at the Cenomanian Aquifer near Jerusalem, Tahal Consult. Eng., Tel Aviv, Israel.

Ben Gai, Y., L. Fleischer, I. Goldberg, M. Gendler, R. Gafsu, H. Gvirtzman, E. Dafny, and J. Steinberg (2007), Structural and lithofacial structure for hydrogeological model of the Yarqon-Taninim Aquifer, 59 pp., Geophys. Inst. of Isr., Lod.

Berger, D. (1999), Hydrological model for the Yarqon Taninim Aquifer, 50 pp., Mekorot, Tel Aviv, Israel.

Carrera-Hernandez, J. J., and S. J. Gaskin (2008), Spatio-temporal analysis of potential aquifer recharge: Application to the basin of Mexico, *J. Hydrol.*, *353*(3–4), 228–246.

Committee on Soil Classification (1979), The classification of Israeli soils, Agric. Res. Organ., Bet Dagan, Israel.

Dafny, E., A. Burg, and H. Gvirtzman (2008a), Pumping influence on the groundwater flow field at the Yarqon-Taninim Groundwater Basin, 89 pp., Isr. Geol. Surv., Jerusalem.

Dafny, E., H. Gvirtzman, and A. Burg (2008b), Numerical model for flow and transport at the Yarqon-Taninim Groundwater Basin, 40 pp., Isr. Geol. Surv., Jerusalem.

Dan, J., and H. Koyumdjisky (1963), The soils of Israel and their distribution, *J. Soil Sci.*, *14*(1), 12–20, doi:10.1111/j.1365-2389.1963.tb00926.x.

Delin, G. N., R. W. Healy, D. L. Lorenz, and J. R. Nimmo (2007), Comparison of local- to regional-scale estimates of ground-water recharge in Minnesota, USA, *J. Hydrol.*, *334*(1–2), 231–249, doi:10.1016/j.jhydrol.2006.10.010.

Dingman, S. L. (1994), *Physical Hydrology*, Prentice Hall, Upper Saddle River, N. J.

Flint, A. L., E. Flint, E. M. Kwicklis, J. T. Fabryka-Martin, and G. S. Bodvarsson (2002), Estimating recharge at Yucca Mountain, Nevada, USA: Comparison of methods, *Hydrogeol. J.*, *10*(1), 180–204, doi:10.1007/s10040-001-0169-1.

Freeze, R., and J. Cherry (1979), Groundwater, 604 pp., Prentice Hall, Englewood Cliffs, N. J.

Frumkin, A., and I. Fischhendler (2005), Morphometry and distribution of isolated caves as a guide for phreatic and confined paleohydrological conditions, *Geomorphology*, *67*(3–4), 457–471, doi:10.1016/j.geomorph.2004.11.009.

Georgakakos, K. P. (2002), Hydrometeorological models for real time rainfall and flow forecasting, in *Mathematical Models of Small Watershed Hydrology and Applications*, edited by V. P. Singh and D. K. Frevert, pp. 593–655, Water Resour. Publ., Highlands Ranch, Colo.

Goldreich, Y. (1998), *The Climate of Israel: Observations, Research and Applications*, 292 pp., Bar Ilan Univ. and Magnes Publ., Ramat Gan, Israel.

Goldshtoff, I. (1972a), Recharge at Yatta, Tahal Consult. Eng., Tel Aviv, Israel.

Goldshtoff, I. (1972b), Recharge at Dahariya, Tahal Consult. Eng., Tel Aviv, Israel.

Goldshtoff, I., and Ben-Zvi (1972), A recharge model for the Y-T basin, Tahal Consult. Eng., Tel Aviv, Israel.

Gregory, L. F. (2006), *Water Budgets and Cave Recharge on Juniper Rangelands in the Edwards Plateau*, 148 pp., Texas A&M Univ., College Station, Tex.

Guttman, J., and D. Zaytun (1996), Flow and salinity model for the Northern Yarqon Taninim Basin, and Taninim Springs, Tahal, Tel Aviv, Israel.

Guttman, J., and H. Zukerman (1995a), Yarqon-Taninim-Beer Sheeba Basin, flow model, 37 pp., Tahal Consult. Eng., Tel Aviv, Israel.

Guttman, J., and H. Zukerman (1995b), Flow model in the eastern basin of the Judea and Samaria Hills, 40 pp., Tahal Consult. Eng., Tel Aviv, Israel.

Guttman, J., I. Goldshtoff, A. Baida, and A. Mercado (1988), A two-layer model of flow regime and salinity in the Yarqon-Taninim Aquifer, 19 pp., Tahal Consult. Eng., Tel Aviv, Israel.

Gvirtzman, H. (2002), Israel water resources, Yad Ben-Zvi, Jerusalem, Israel.

Hughes, A. G., M. M. Mansour, and N. S. Robins (2008), Evaluation of distributed recharge in an upland semi-arid karst system: The West Bank Mountain Aquifer, Middle East, *Hydrogeol. J.*, *16*(5), 845–854, doi:10.1007/s10040-008-0273-6.

Israel Hydrological Service (IHS) (2008), Summary of the 2007/08 rain year, hydrological characteristics, 46 pp., Isr. Hydrol. Serv., Jerusalem.

Khazaei, E., A. E. F. Spink, and J. W. Warner (2003), A catchment water balance model for estimating groundwater recharge in arid and semiarid regions of south-east Iran, *Hydrogeol. J.*, *11*(3), 333–342.

Kurtzman, D., S. Navon, and E. Morin (2009), Improving interpolation of daily precipitation for hydrologic modelling: Spatial patterns of preferred interpolators, *Hydrol. Processes*, *23*(23), 3281–3291.

Lee, C. H., W. P. Chen, and R. H. Lee (2006), Estimation of groundwater recharge using water balance coupled with base-flow-record estimation and stable-base-flow analysis, *Environ. Geol.*, *51*(1), 73–82, doi:10.1007/s00254-006-0305-2.

Lundqvist, J., and P. Gleick (2000), Sustaining our waters into the 21st century, Stockholm Environ. Inst., Sweden.

Natan, E. (2001), Distribution of karst phenomena in north-eastern Samaria and implications on contamination of the mountain aquifer, Israel, Hebrew Univ. of Jerusalem, Israel.

Rajmohan, N., A. Al-Futaisi, and A. Jamrah (2007), Evaluation of long-term groundwater level data in regular monitoring wells, Barka, Sultanate of Oman, *Hydrol. Processes*, *21*(24), 3367–3379, doi:10.1002/hyp.6543.

Rimmer, A., and Y. Salingar (2006), Modelling precipitation-streamflow processes in karst basin: The case of the Jordan River sources, Israel, *J. Hydrol.*, *331*(3–4), 524–542, doi:10.1016/j.jhydrol.2006.06.003.

Scanlon, B. R., and P. G. Cook (2002), Theme issue on groundwater recharge: Preface, *Hydrogeol. J.*, *10*(1), 3–4, doi:10.1007/s10040-001-0175-3.

Scanlon, B. R., R. W. Healy, and P. G. Cook (2002), Choosing appropriate techniques for quantifying groundwater recharge, *Hydrogeol. J.*, *10*(2), 347–347, doi:10.1007/s10040-002-0200-1.

Scanlon, B. R., K. E. Keese, A. L. Flint, L. E. Flint, C. B. Gaye, W. M. Edmunds, and I. Simmers (2006), Global synthesis of groundwater recharge in semiarid and arid regions, *Hydrol. Processes*, *20*(15), 3335–3370, doi:10.1002/hyp.6335.

Shah, T., D. Molden, R. Sakthivadivel, and D. Seckler (2000), The global groundwater situation: Overview of opportunities and challenges, Int. Water Manage. Inst., Colombo, Sri Lanka.

Sheffer, N. A. (2009), Variable scale recharge measurement and modelling using the hydrometeorological DREAM, Ph.D. dissertation, 97 pp, Hebrew Univ. of Jerusalem, Israel.

Sheffer, N. A., M. Cohen, E. Morin, T. Grodek, A. Gimburg, H. Gvirtzman, and A. Frumkin (2008), Direct measurements of epikarst percolation in a dry Mediterranean environment, Sif Cave, Israel, *Eos Trans. AGU*, *89*(23), Jt. Assem. Suppl., Abstract H33D-03.

Singer, A., U. Schwertmann, and J. Friedl (1998), Iron oxide mineralogy of terra rossa and rendzinas in relation to their moisture and temperature regimes, *Eur. J. Soil Sci.*, *49*(3), 385–395, doi:10.1046/j.1365-2389.1998.4930385.x.

Sophocleous, M. A. (2004), Groundwater recharge and water budget of the Kansas High Plains and related aquifers, *Kans. Geol. Surv. Bull.*, *249*, 1–10.

Sophocleous, M. (2005), Groundwater recharge and sustainability in the High Plains Aquifer in Kansas, USA, *Hydrogeol. J.*, *13*(2), 351–365, doi:10.1007/s10040-004-0385-6.

Szilagyi, J., F. E. Harvey, and J. F. Ayers (2005), Regional estimation of total recharge to ground water in Nebraska, *Ground Water*, *43*(1), 63–69, doi:10.1111/j.1745-6584.2005.tb02286.x.

Tindall, J., and J. Kunkel (1999), *Unsaturated Zone Hydrology for Scientists and Engineers*, 624 pp., Prentice Hall, Upper Saddle River, N. J.

Vorosmarty, C. J., P. Green, J. Salisbury, and R. B. Lammers (2000), Global water resources: Vulnerability from climate change acid population growth, *Science*, *289*(5477), 284–288, doi:10.1126/science.289.5477.284.

Wilcox, B. P., C. Munster, L. F. Gregory, B. Shade, M. K. Owens, and G. Veni (2008), Recharge on karst shrublands: Insights from cave hydrology and large scale rainfall experiments, *Eos Trans. AGU*, *89*(23), Jt. Assem. Suppl., Abstract H34A-05.

Zukerman, H. (1999), The Yarqon-Taninim Basin. Flow model update, 11 pp., Tahal, Tel Aviv, Israel.

E. Dafny and H. Gvirtzman, Institute of Earth Sciences, Hebrew University of Jerusalem, Edmond J. Safra Campus, Givat Ram, Jerusalem 91904, Israel.

A. Frumkin, E. Morin, and S. Navon, Department of Geography, Hebrew University of Jerusalem, Mount Scopus, Jerusalem 91905, Israel.

N. A. Sheffer, Bureau of Economic Geology, University of Texas at Austin, University Station, Box X, Austin, TX 78713, USA. (nathan.sheffer@beg.utexas.edu)